ACCSCIENCE PUBLISHING

International Journal of Bioprinting

RESEARCH ARTICLE

3D-bioprinted placenta-on-a-chip platform for modeling the human maternal–fetal barrier

Yazhi Sun[1†], Henry H. Hwang[1†], Chandana Tekkatte[2,3†], Scott A. Lindsay[2,3], Anelizze Castro-Martinez[2,3], Claire Yu[1], Isabella Saldana[2,3], Xuanyi Ma[1], Omar Farah[3,4], Mana M. Parast[3,4], Louise C. Laurent[2,3*], and Shaochen Chen[1*]

[1]Department of Chemical and Nano Engineering, University of California San Diego, San Diego, CA, United States of America

[2]Department of Obstetrics, Gynecology, and Reproductive Sciences, University of California San Diego, San Diego, CA, United States of America

[3]Sanford Consortium for Regenerative Medicine, University of California San Diego, San Diego, CA, United States of America

[4]Department of Pathology, University of California San Diego, San Diego, CA, United States of America

Abstract

The placenta plays a vital role in pregnancy by regulating selective exchange between the maternal and fetal circulations and producing essential hormonal signals. In this study, we present an *in vitro* placenta-on-a-chip platform that leverages 3D bioprinting to replicate the structural and functional features of the human placental barrier. This microengineered system utilizes digital light processing-based 3D bioprinting to fabricate the microfluidic mold and construct 3D encapsulated cell cultures within a biomimetic hydrogel scaffold, enabling co-culture of three human cell types, including two derived from primary placental tissue. The system demonstrated excellent cell viability, high metabolic activity, placental hormone secretion, and native-like selective barrier transport properties. This system offers a versatile platform for experimental perturbations to explore mechanisms of normal placental function and identify contributors to placental dysfunction.

Keywords: Bioprinting; Microfluidics; Microphysiological system; Organ-on-a-chip; Placenta; Trophoblast stem cells

1. Introduction

The human placenta acts as a vital interface mediating the exchange of nutrients, gases, and waste products between the maternal and fetal compartments, while also producing key hormones essential for maintaining pregnancy. It plays a crucial role in fetal health, not only in supporting fetal growth and development but also serving as a barrier to exogenous factors, such as environmental pollutants, pharmaceutical compounds, and pathogens. Notably, about 90% of women take at least one medication during their pregnancy,[1,2] underscoring the urgent need for placental models that can be used to evaluate whether and how these new medications can cross over into the fetal circulation.

†These authors contributed equally to this work.

***Corresponding authors:**
Louise C. Laurent (llaurent@ucsd.edu)

Shaochen Chen (shc064@ucsd.edu)

Citation: Sun Y, Hwang HH, Tekkatte C, *et al*. 3D-bioprinted placenta-on-a-chip platform for modeling the human maternal–fetal barrier. *Int J Bioprint*. 2025;11(5):178-196. doi: 10.36922/IJB025270262

Received: July 2, 2025
Revised: July 22, 2025
Accepted: July 28, 2025
Published Online: July 28, 2025

The functional units of the human placenta are the chorionic villi—finger-like structures that extend from the fetal tissue into the maternal blood space, allowing close contact between fetal capillaries and maternal blood (Figure 1A). Chorionic villi serve as the primary interface for gas and nutrient exchange between the maternal and fetal circulations. Each villus consists of an outer layer of syncytiotrophoblast (STB) and an interior filled with stromal connective tissue, resident stromal cells, and a variably distributed network of fetal capillaries. The villi are bathed in maternal blood within the intervillous space, allowing direct contact between maternal blood and the STB surface. This close proximity to the fetal capillaries facilitates efficient exchange of gases, nutrients, and waste products between the maternal and fetal circulations.

Several existing strategies have been developed to study placental function, but each has important limitations. For example, 2D cell culture models fail to replicate the complex interactions between different cell types and the influence of blood flow present in the placenta. *Ex vivo* perfusion of the human placenta preserves the complex tissue architecture, but often lacks accurate representation of the *in vivo* flow environment, and is hampered by low throughput, donor variability, and scarcity.[3–5] Animal models, while useful for *in vivo* studies, have limited relevance to human physiology due to cross-species differences in placental morphology and cellular composition.[6,7] Studies involving pregnant women are constrained by ethical, safety, and logistical concerns. In contrast, *in vitro* microfluidic and microphysiological systems offer key advantages, including standardized fabrication, the ability to mimic tissue architecture and support long-term culture, physiological relevance, and precise experimental control.[8]

Recent *in vitro* microfluidic models have sought to recapitulate the physiological and functional aspects of these structures. To simulate the fetal-maternal interface, many studies employ synthetic porous membranes,[9,10] such as commercial Transwell inserts (Corning), or natural materials like vitrified collagen and Matrigel,[11,12] which serve to separate the two compartments, with cells seeded accordingly. While these studies demonstrated some placental functions, such as drug transport, the placental cells used were often immortalized lines derived from cancerous placental cells ("choriocarcinomas"), resulting in behavior and expression profiles markedly different from healthy placental cells.[13] Advanced microfluidics-based platforms have also been used as a more intricate and dynamic approach to model the multi-cellular interactions in the placental villus. Some of these systems incorporated primary or induced pluripotent stem cell-derived placental cells; however, they generally relied on monolayer cell seeding, rather than mimicking the 3D *in vivo* architecture.[14–16] One recent study utilized trophoblast organoids to establish a 3D culture, but the spherical organoids did not fully cover the interface and lacked the inclusion of other relevant cell types and intercellular interactions.[17] Moreover, a major challenge in recapitulating human placental physiology with microfluidics is the enclosed chamber design, which complicates patterning multiple cell types into organized structures that mimic native placental architecture. Although sequential perfusion of different cell types into chambers is possible, the resulting 2D cultures fail to reproduce the 3D *in vivo* environment. Thus, an *in vitro* system that mimics the 3D structure and functionality of the human chorionic villus remains to be developed with primary cells for investigation of drug transport across this barrier in the setting of normal pregnancy and disease.

Currently, most placenta-on-a-chip platforms require photolithography for microfluidic device fabrication, which is time-consuming, labor-intensive, and dependent on expensive cleanroom infrastructure.[18–20] In contrast, digital light processing (DLP)-based 3D printing offers a rapid, cost-effective, and mask-free alternative for fabricating microfluidic molds with high spatial resolution. By projecting patterned light onto photopolymerizable materials, DLP 3D printing enables the precise creation of high-resolution geometries directly from digital designs, thereby streamlining the microfabrication process for the master molds. In addition, it has also been widely adopted in 3D cell culture and tissue engineering, where it supports the fabrication of cell-laden hydrogels and organ-on-a-chip platforms with tunable architecture and mechanical properties.[21,22] Its versatility makes DLP 3D printing an ideal tool for developing physiologically relevant *in vitro* models.

In this study, we present a novel human placenta-on-a-chip (hPOC) microfluidic system featuring primary placental cell tri-coculture within a "hybrid" open/closed microfluidic design (Figure 1B–D). The device contains dual compartments separated by a porous membrane that provides structural support for both the maternal compartment and fetal capillaries. This configuration recapitulates the spatial organization of the chorionic villus. On the maternal side, primary human trophoblast stem cells (hTSCs) are cultured on the membrane-facing surface, with placenta-derived stromal fibroblasts (PDSFs) embedded in a methacrylated gelatin (GelMA) layer beneath them by DLP bioprinting. On the fetal side, primary human umbilical vein endothelial cells (HUVECs) are seeded on the underside of the membrane and maintained under continuous perfusion to simulate dynamic fetal circulation.

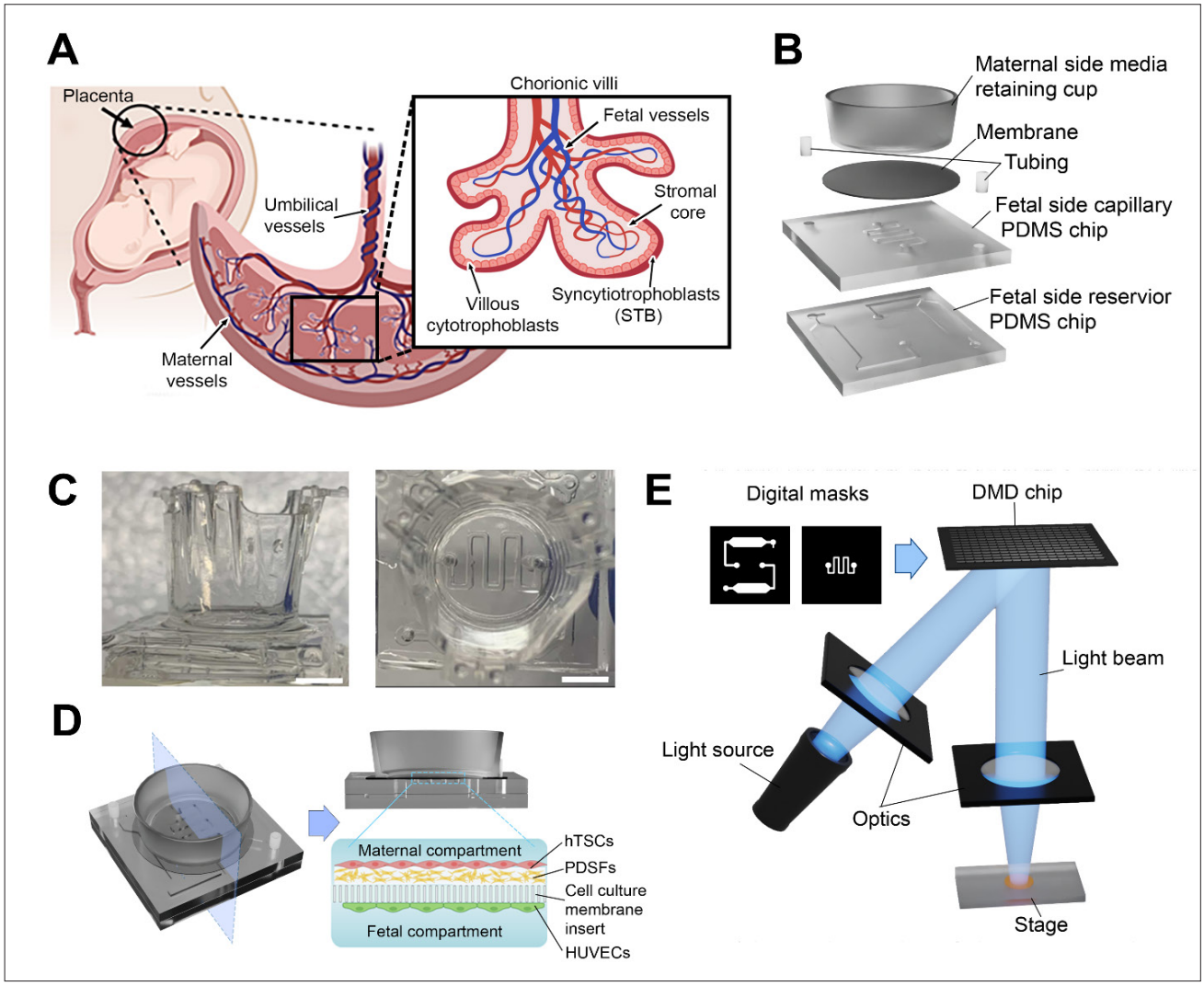

Figure 1. Schematic of the human placenta and the hPOC design. (A) Illustration of the human placenta, featuring the chorionic villi, which mediate nutrient and gas exchange at the maternal-fetal interface. (B) Exploded view of the hPOC device components, highlighting the porous membrane that separates the maternal and fetal compartments. (C) Side view (C, left) and top view (C, right) of the assembled hPOC device. Scale bar: 5 mm. (D) Cross-sectional schematic of the assembled hPOC device, displaying the multi-layered cellular architecture that recapitulates key features of the placental barrier. (E) Schematic of DLP bioprinting. Digital masks are projected via a DMD onto the sample stage, selectively solidifying the polymer precursor to create patterned structures. Abbreviations: DLP, digital light processing; DMD, digital mirror device; hPOC, human placenta-on-a-chip; hTSCs, human trophoblast stem cells; HUVECs, human umbilical vein endothelial cells; PDMS, polydimethylsiloxane; PDSFs, placenta-derived stromal fibroblasts.

We employed DLP 3D printing (Figure 1E) to fabricate the master molds of the microfluidic chambers for polydimethylsiloxane (PDMS) casting. This enabled assembly of the hPOC device with an open media-retaining cup and enclosed microfluidic channels. After extensive optimization of cell attachment and viability of the primary placental cell types on 3D-printed hydrogel scaffolds with varying stiffness, we identified optimal stiffness, culture, and flow conditions for device assembly. The three cell types were systematically seeded into the 3D tri-coculture model to test functional transport properties. Our results demonstrated that the hPOC device produces placental hormones and mimics key placental barrier and transport functions, suggesting utility in applications such as drug/nutrient transport. To the best of our knowledge, this open/closed microfluidic design is the first system incorporating primary placenta-derived cells alongside primary endothelial cells in a tri-coculture configuration. This setup offers the capability to support both genetic and environmental manipulations, providing a versatile platform for future studies of human placental transport and function.

2. Materials and methods

2.1. hPOC device fabrication

The microfluidic architecture was designed using computer-aided design software (AutoCAD, Autodesk, USA). The photocrosslinkable hydrogel, poly(ethylene glycol) diacrylate (PEGDA; molecular weight [MW]: 250 Da) and the photoinitiator phenyl bis(2,4,6-trimethylbenzoyl) phosphine oxide (trade name: Irgacure-819, BASF) were obtained from Sigma Aldrich (USA). The polymer precursor consisted of PEGDA 250 and 1% (w/v) Irgacure-819.

An in-house DLP 3D printer was utilized to fabricate positive master molds for both the microfluidic fetal capillary compartment and fluid reservoirs. After printing, the molds were rinsed with isopropanol to remove any uncrosslinked PEGDA, which would otherwise inhibit the crosslinking of PDMS.

PDMS was prepared by mixing the curing agent and base monomer at a 1:10 mass ratio, poured over the master molds, degassed, and cured overnight at 80°C. Once cured, the PDMS chips containing the fetal capillary and fluidic reservoir features were demolded, cut, and ported. The fluidic reservoir component was bonded to a glass slide using oxygen plasma treatment, and the fetal capillary component was aligned and affixed atop the reservoir using a thin layer of PDMS glue.

To form the membrane separating the fetal and maternal compartments, a commercially available cell culture insert membrane (polyethylene terephthalate with 3 μm pores, cellQART, Germany) was used. A 1:1 mixture of toluene and standard-mix PDMS was spin-coated onto a glass slide (60 s, 1500 rpm) to serve as an adhesive, after which the fetal side of the partially assembled device was gently stamped onto the spin-coated slide, ensuring coating of the negative spaces without obstructing channel patency.

The membrane was aligned and placed atop the fetal capillary compartment and cured for 10 min at 80°C. Finally, the retaining cup from the cell culture insert was bonded atop the membrane using additional PDMS, completing the maternal compartment of the hPOC device.

2.2. Cell culture

2.2.1. Primary placenta-derived stromal fibroblasts

The current study involving human-sourced tissues used in biomedical research was approved by the Institutional Review Board at the University of California San Diego (IRB #181917). Following written informed consent from donors, third-trimester placentas (gestational age: 36–38 weeks) from uncomplicated pregnancies were collected and transported to the laboratory on ice within 1 h of delivery.

Primary PDSFs were isolated from placental chorionic villi using the explant culture method, as previously described by Igura et al.[23] Briefly, the basal and chorionic plates were excised using sterile surgical scissors and discarded to eliminate maternal cell contamination. Lobes of placental villi were then dissected, carefully avoiding large blood vessels, and rinsed thoroughly in sterile phosphate-buffered saline (PBS) to remove maternal blood. Villus chunks were placed in a petri dish containing pre-warmed Dulbecco's Modified Eagle Medium (DMEM)-high glucose medium and dissected into 7–10 mm explants.

A total of 10 explants were transferred to a 10 cm tissue culture-treated dish and allowed to adhere by drying at room temperature for 1 h. Once firmly attached, 15 mL of pre-warmed growth medium (DMEM-high glucose supplemented with 10% fetal bovine serum (FBS) and 1% penicillin–streptomycin) was gently added to the side of each dish to avoid dislodging the explants. Cultures were maintained in a humidified incubator at 37°C and 5% CO_2 under normoxic conditions for up to 4 weeks. During this time, PDSFs migrated out of the cut surfaces of the explants. Growth medium was replenished every 3–4 days (Figure S1). Migrated cells were harvested using 0.05% trypsin-EDTA solution (3 min at 37°C), expanded in culture, and cryopreserved in liquid nitrogen for future use. All encapsulated cells used in this study were within 12 population doublings (approximately four to six passages).

2.2.2. Human trophoblast stem cells

We used a hTSC line (1049) that was established from early gestation (gestational age: 6–8 weeks) placentas, as previously described by Okae et al.[24] The use of early gestation placental tissues in this study was approved by the Institutional Review Board of the University of California, San Diego (IRB #172111). Written informed consent was obtained from all donors. Cells were routinely maintained on tissue culture plates coated with 5 μg/mL collagen-IV (C0543-1VL, Sigma-Aldrich, USA) in iCTB medium,[25] modified from the medium used by Okae et al.[24] hTSC media, consisting of Advanced DMEM/F12 supplemented with 1× N2 and 1× B27 supplements, 2 mM glutamine, 150 μM 1-thioglycerol, 0.05% of 30% BSA solution, and 1× Knockout Serum Replacement (KSR). The medium was further supplemented with 2 μM CHIR99021, 500 nM A83-01, 1 μM SB431542, 5 μM Y-27632, 0.8 mM valproic acid sodium salt, 100 ng/mL FGF2, 50 ng/mL EGF, 20 ng/mL Noggin, and 50 ng/mL HGF.

To induce differentiation into multinucleated STB, hTSCs were switched to STB differentiation medium, as per the protocol by Okae et al.,[24] composed of DMEM/F12 (without HEPES), supplemented with 1× ITS-X, 3.2% KSR, 1% of 30% BSA solution, 0.1 mM beta-mercaptoethanol,

2.5 μM Y27632, and 2 μM forskolin. For the tri-coculture experiments, primary hTSCs between passages 35 and 40 were used for syncytialization.

2.2.3. Human umbilical vein endothelial cells

HUVECs were obtained from the American Type Culture Collection (USA) and expanded in standard 2D culture using EGM-2 endothelial cell growth medium supplemented with 2% FBS and vascular endothelial growth factor (Lonza, USA). Prior to seeding into the microfluidic device, HUVECs were cultured under these conditions to ensure optimal cell health and expansion. HUVECs used for the tri-coculture experiments were between passages 3 and 5.

During static culture within the device, media were manually replenished daily. Once perfusion was initiated, continuous media flow was maintained to support endothelial maturation and viability.

2.3. Tri-coculture assembly and functional characterization

2.3.1. Sequential cell seeding and culture timeline

Prior to cell culture, both the fetal and maternal compartments of the device were incubated at 37°C overnight with a solution containing 5 μg/mL rat tail collagen type I (354236, Corning, USA) and a 1:25 dilution of bovine plasma-derived fibronectin (F1141, Sigma-Aldrich, USA) in 1× DPBS to promote cellular attachment.

On day 0, a PDSF layer was established in the maternal compartment using a GelMA-based bioink. GelMA was synthesized as previously described[26] and used at 7.5% (v/v) in 1× DPBS. The photoinitiator lithium phenyl-2,4,6-trimethylbenzoylphosphinate (LAP, Tokyo Chemistry Industry, Japan) was added at 0.6% (v/v). DiD (Vybrant™, Thermo Fisher, USA)-stained PDSFs were encapsulated within the GelMA bioink at a density of 75,000 cells/mL and carefully layered onto the membrane "floor" of the maternal compartment using PDMS spacers (125 μm thick) to constrain hydrogel thickness. The construct was crosslinked using UV light from the DLP 3D printer. After polymerization, the PDMS spacers were carefully removed, leaving the GelMA-encapsulated PDSF layer intact and adhered to the membrane.

On day 1, green fluorescent protein (GFP)-expressing HUVECs were seeded into the fetal compartment at a density of approximately 8×10^6 cells/mL and statically cultured for 3 days. Media in the fetal compartment were replenished daily through the reservoir.

On day 4, approximately 500,000 red fluorescent protein (RFP)-expressing hTSCs were suspension-seeded into the maternal compartment atop the PDSF-encapsulated GelMA layer. Gravity-assisted sedimentation facilitated their attachment. hTSCs were cultured in iCTB media for 24 h.

On day 5, the media in the maternal compartment were switched to STB differentiation media. On the same day, perfusion of the fetal compartment was initiated using a peristaltic pump (PeriWave Micro, CorSolutions, USA) at a volumetric flow rate of 3.5 μL/min. This perfusion continued for 3 days, and the media outflow was collected every 24 h. Maternal supernatant was also collected daily, and media in the maternal compartment were replaced with fresh STB differentiation media.

On day 8, after 3 days of syncytialization and perfusion, assays to assess placental barrier formation and function—including cell viability, fluorescent molecule transport, and imaging—were performed.

2.3.2. Mechanical measurement of GelMA constructs

Cylindrical GelMA hydrogel samples (1 mm diameter × 1 mm height) were bioprinted using the designated light exposure parameters. The Young's modulus was measured using a Microtester system (CellScale, USA). Samples were compressed to 20% strain using a cantilever with a platen tip at a rate of 8 μm/s, held for 2 s, then allowed to recover. Strain and force were recorded, and the Young's modulus was calculated using a custom MATLAB script.

2.3.3. LIVE/DEAD™ staining

Cell viability was assessed using the LIVE/DEAD® Viability/Cytotoxicity Kit (Invitrogen, USA), which employs calcein AM (2 μM, 1:2000 dilution) to label live cells green and propidium iodide (4 μM, 1:500 dilution) to stain dead cells red. Cells were incubated with the dye mixture in serum-free media for 30 min at 37°C and 5% CO_2. Following incubation, cultures were washed with fresh media to eliminate excess dye and imaged using a Leica DMI6000B fluorescence microscope (Leica Microsystems, Germany).

2.3.4. XTT viability assay

Cell metabolic activity was quantified using the CyQUANT XTT Cell Viability Assay Kit (Invitrogen, USA). A working solution was prepared by mixing 5 mL of XTT labeling reagent with 0.1 mL of the electron-coupling reagent. The solution was added to both maternal and fetal compartments to a final XTT concentration of 0.3 mg/mL. Supernatant samples were collected every 15 min for 3 h, and absorbance was measured using a microplate reader (Tecan Infinite 200 Pro, Tecan Trading AG, Switzerland) at 450 nm with a reference wavelength of 650 nm.

2.3.5. Quantification of placenta-specific hormones via ELISA

Supernatant samples collected daily from the maternal and fetal compartments following hTSC seeding were analyzed for placenta-specific hormone secretion using enzyme-linked immunosorbent assays (ELISAs), following the manufacturer's protocols for each kit. Estradiol levels were measured using the Estradiol Human ELISA Kit (KAQ0621, Thermo Scientific, USA). Human placental lactogen (hPL) was quantified using the Human CSH1 Placental Lactogen Sandwich ELISA Kit (LS-F16356, LSBio, USA). Beta subunit human chorionic gonadotropin (hCGβ) was assessed using the Human Chorionic Gonadotropin ELISA Kit (HC251F, Calbiotech, USA). Progesterone was measured using the Progesterone Competitive ELISA Kit (EIAP4C21, Invitrogen, USA).

2.3.6. Imaging and morphological characterization

An upright fluorescence microscope with a motorized stage (Leica DMI6000B, Leica Microsystems, Germany) and stage-top cell culture incubator (Tokai Hit INU, Tokai Hit, USA) was used for live imaging of the tri-coculture system during the first 24 h of perfusion. Fluorescent tile scans (5×) were acquired at defined time points across multiple channels and stitched into mosaic images using the onboard LAS-X software (Leica, Germany). For 3D imaging, a ZEISS LSM 880 Confocal with FAST Airyscan (ZEISS, Germany) was used to capture Z-stacks of the PDSF-encapsulated GelMA hydrogels and the materno-fetal barrier in the tri-coculture model, which were processed into maximum projections using ZEISS Airyscan Software or 3D reconstructions using Imaris (Oxford Instruments, UK).

2.4. Assessment of barrier integrity and molecular permeability

2.4.1. Sodium fluorescein permeability

Sodium fluorescein salt (Na-F; Sigma-Aldrich, USA) was used as a tracer molecule to assess passive permeability across the placental barrier. A working solution of Na-F (40 ng/mL; 100 nM) was introduced to the maternal compartment. After 24 h, samples were collected from the fetal compartment and analyzed using a microplate reader (Tecan Infinite 200 Pro, Tecan Trading AG, Switzerland) with excitation at 485 nm and emission at 528 nm. The assay was performed on four types of devices: Type 1 was an acellular device; Type 2 included an acellular GelMA layer; Type 3 incorporated HUVECs on the fetal side; and Type 4 represented the full tri-coculture system. The concentration of 40 ng/mL was selected based on preliminary experiments, which demonstrated that higher concentrations, such as 2 μg/mL, resulted in excessive nonspecific staining of the polyethylene terephthalate (PET) membrane.

2.4.2. FITC-conjugated dextran permeability

FITC-conjugated dextran (FITC-dextran) was introduced into the maternal compartment at a concentration of 1 mg/mL in STB media. After 24 h, samples from the fetal compartment were collected and analyzed using a microplate reader (Tecan Infinite 200 Pro, Tecan Trading AG, Switzerland) with excitation at 490 nm and emission at 520 nm. The assay was performed on four types of devices: Type 1 was an acellular device; Type 2 included an acellular GelMA layer; Type 3 incorporated HUVECs on the fetal side; and Type 4 represented the full tri-coculture system.

2.4.3. Glucose transport

To assess glucose transfer across the tri-coculture model, media containing glucose (STB media in the maternal compartment and EGM-2 media in the fetal compartment) were used. The maternal and fetal compartments initially contained approximately 300 mg/dL and 100 mg/dL glucose, respectively. Samples were collected from both compartments at defined time points and analyzed using a commercial glucose monitoring system (GlucCELL, Chemglass Life Sciences, USA). These measurements were conducted in both tri-coculture devices and control devices containing acellular membranes to assess baseline permeability.

2.5. Statistical analysis

All data are presented as mean ± standard deviation, unless otherwise noted. Statistical analyses and graphical representations were performed using GraphPad Prism software (GraphPad Software, USA). Paired *t*-tests were used to assess differences between the fetal and maternal sides in Figure 4. One-way analysis of variance (ANOVA) was used to assess differences among multiple groups for other figures. Statistical significance was defined as $^{*}p < 0.05$, $^{**}p < 0.01$, $^{***}p < 0.001$, and $^{****}p < 0.0001$.

3. Results

3.1. Fabrication of the hPOC device

Figure 1B displays the schematic of the hPOC device design, and Figure S2 features the cross-sectional view. The hPOC device was constructed through a multi-step process: to model the fetal capillary compartment, a serpentine microchannel (500 μm diameter) was fabricated using DLP 3D printing. Two digital masks were projected onto a PEGDA resin to create a mold directly on glass coverslips. PDMS was then cast onto this mold to form the fetal capillary chip, which was adhered to the underside of a porous membrane with the serpentine pattern facing upward. Four access ports were punched in the PDMS to

allow for media inflow, outflow, and connection to the fetal media reservoir. A separate reservoir chip was then aligned and bonded to the fetal capillary chip, and tubing was inserted into two diagonal ports to enable perfusion. On the maternal side, a plastic reservoir cup was affixed atop the porous membrane using a thin layer of PDMS glue to complete the assembly. This configuration supports static culture, with culture media retained within the cup. In contrast, the fetal side supports dynamic culture through continuous media perfusion: media is introduced via the inlet tubing, flows through the reservoir layer, and is directed into the fetal capillary compartment.

The hPOC device incorporates two primary placenta-derived cell lines—hTSCs and PDSFs—along with HUVECs derived from the human umbilical vein endothelium, to represent key structural components of the human placental villus (Figure 1A and D). In the maternal compartment, PDSFs are first encapsulated in a 125 μm GelMA layer on top of the porous membrane, followed by seeding of hTSCs, which are induced to differentiate to STB (hTSC–STB), mimicking the native arrangement of trophoblasts overlaying the stromal core. On the fetal side, HUVECs are seeded onto the inner surface of the serpentine microchannel beneath the membrane, representing the fetal capillary endothelium. While the perfusable fetal compartment enables dynamic culture with continuous media flow, an initial period of static culture is necessary to promote HUVEC adhesion. During this period of static culture, the reservoir permits sufficient passive diffusion to support cell viability. Our novel multi-layer design enables interaction between the maternal and fetal compartments through an engineered placental barrier comprised of hTSC–STB, PDSFs, a porous membrane, and HUVECs, with transport driven by gravity and diffusion. Additionally, the design recapitulates the physiological relationship between maternal and fetal blood spaces: a larger maternal surface area and fine fetal capillary channels mimic the natural arrangement in which maternal blood in the intervillous space surrounds the chorionic villi, offering greater exchange surface area and blood volume relative to the fetal capillary network within each villus.

3.2. Optimization of cell culture in the maternal compartment

To optimize the maternal compartment, we first established culture conditions for PDSFs encapsulated in a 125 μm-thick GelMA slab. This thickness approximates the physiological thickness of the stromal layer in the human placenta and enables adequate nutrient diffusion to support the 3D culture of PDSFs. The growth and morphology of PDSFs are influenced by the stiffness of the surrounding matrix. Utilizing DLP bioprinting, we are able to tune the bulk stiffness of the hydrogel network by adjusting the light exposure,[21] achieving stiffnesses ranging from ~1.5 to ~30 kPa (Figure S3). We assessed the viability of PDSFs encapsulated in GelMA at stiffness levels of ~1.5, ~7, and ~18 kPa (Figure 2A). PDSFs maintained high viability across this range of stiffness; however, we selected the GelMA stiffness of ~18 kPa for subsequent experiments based on cellular morphology, as cells exhibited more pronounced elongated processes characteristic of fibroblasts at this higher stiffness level.

We then assessed the viability, morphology, and growth of hTSCs as a function of GelMA stiffness. Figure 2B presents hTSCs cultured on printed GelMA scaffolds spanning the same stiffness range used for PDSF encapsulation. Live/dead viability staining and fluorescence imaging demonstrated excellent viability and typical hTSC morphology across the range of stiffness, including the previously identified optimal stiffness of ~18 kPa.

During gestation, the placenta undergoes significant structural remodeling, including the syncytialization of cytotrophoblasts (CTB), forming large, multinucleated STB on the maternal side of the chorionic villi.[27] This transformation is a defining feature of the placental barrier and is widely regarded as essential to replicate in any *in vitro* chorionic villus model.[28] In many such models, syncytialization of mononuclear CTB-like cells (such as those from the BeWo choriocarcinoma cell line) is induced by treatment with forskolin, which elevates intracellular cyclic adenosine monophosphate (cAMP) levels. The rise in cAMP activates protein kinase A and other downstream signaling molecules that regulate the expression of proteins and enzymes involved in cell-cell adhesion and membrane fusion, driving the formation of STBs.[29] To induce syncytialization, hTSCs seeded on ~18 kPa GelMA scaffolds were cultured in forskolin-containing media. After 72 h, the cells were stained with wheat germ agglutinin to evaluate cell borders and DAPI to mark nuclei, revealing complete coverage of the culture surface and a high degree of syncytialization (Figure 2C). The ability of the GelMA scaffold to support a high density of hTSC growth and syncytialization is critically important, as these are essential to mimicking the integrity of the placental barrier.

3.3. Optimization of HUVEC culture in the fetal compartment

We optimized the culture conditions for HUVECs in the microchannels of the fetal compartment. While hTSCs could adhere readily to the GelMA surface on the maternal side due to intrinsic cell-binding motifs in GelMA,[30] seeding HUVECs on the fetal side was

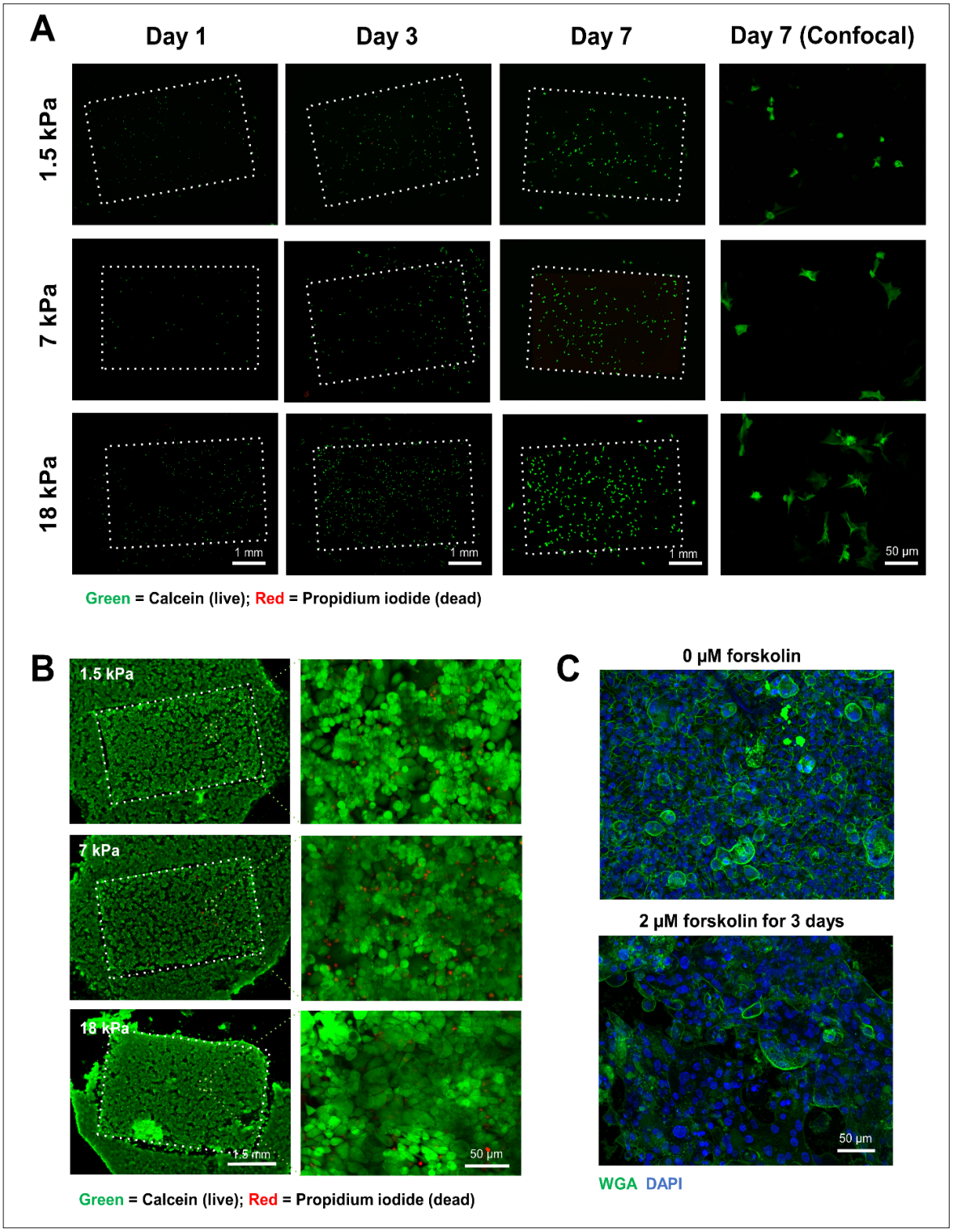

Figure 2. Optimization of cell culture conditions in the maternal compartment. (A) Live/dead staining of placental-derived stromal fibroblasts (PDSFs) encapsulated in methacrylated gelatin (GelMA) hydrogels and cultured over 7 days. (B) Live/dead staining of human trophoblast stem cells (hTSCs) cultured atop 3D-printed GelMA scaffolds for 7 days. (C) Confocal microscopy images of hTSCs stained with wheat germ agglutinin (WGA, cell membrane) and DAPI (nuclei): cells cultured in standard media (C, top) and cells treated with forskolin-containing media for 3 days to induce syncytialization (C, bottom). Scale bars: 1.5 mm (B, left); 1.0 mm (A, far-left, left-middle, right-middle); 50 μm (A, far-right; B, right; C).

more challenging. The synthetic cell culture insert lacks natural extracellular matrix (ECM) ligands and does not inherently support effective cell adhesion. To enhance attachment, both maternal and fetal compartments were pre-treated with bovine plasma-derived fibronectin and collagen-I for overnight incubation prior to HUVEC seeding, consequently promoting cell adhesion within the microchannels and on the fetal-side membrane surface. We then inverted the hPOC device, seeded HUVECs at a density of 1×10^6 cells/mL on the fetal side membrane through the channel, and incubated the device for 1 h to allow for cell adhesion. The devices were then returned to an upright position and connected to the media-filled reservoir. In an initial experiment, we examined HUVEC viability inside the 500 μm-wide microchannels in static culture over the course of 72 h using live/dead staining (Figure 3A), with daily imaging. While a slight increase in dead cells was observed over the 3 days of static culture (Figure 3A**, inset**), the vast majority of HUVECs remained viable at the end of the experiment.

In the second experiment, we used GFP-labeled HUVECs for the main co-culture experiments to facilitate monitoring of HUVEC morphology under perfusion and quantified cell circularity and area over time. As displayed in Figure 3B, GFP-HUVECs exhibited a rounded, highly circular morphology immediately post-seeding, indicative of seeding stress. A day after static culture in the microchannels, the cells spread out and exhibited increased area as they flattened, while maintaining the characteristic "cobblestone" morphology typically observed in static culture. After 1 day of perfusion culture, GFP-HUVECs began to adopt a more elongated, striated morphology, reflecting their response to shear forces within the microchannel. Quantitative image analysis confirmed these observations: by day 2, HUVEC circularity markedly decreased while cell area increased (Figure 3C and D), consistent with the morphological transition induced by perfusion.

3.4. Tri-coculture assembly of maternal and fetal compartments

The assembly of the complete tri-coculture device was carefully designed to allow sufficient time for cell adhesion, proliferation, and functionality of the placental barrier (Figure 4A). The three cell types (PDSFs, GFP-HUVECs, and RFP-labeled hTSCs) were seeded according to a staggered timeline (Figure 4A) to ensure that optimal cell viability, cell density, and functionality were achieved.

Following the previously optimized conditions for each cell type, we began the tri-coculture assembly with DLP 3D bioprinting of the GelMA-encapsulated PDSFs on day 0. On the following day, GFP-HUVECs were seeded into the fetal compartment with care to avoid drying the PDSF-containing GelMA layer in the maternal compartment. After incubation, the device was returned to its upright orientation; fresh PDSF growth media was introduced into the maternal compartment, and the reservoir with HUVEC growth media was connected to the fetal compartment. The system was maintained under static culture for 3 days to allow for initial cell proliferation and stabilization. On day 3, the PDSF-encapsulated GelMA layer in the maternal chamber was coated with collagen and fibronectin to prepare the surface for hTSC seeding the following day. On day 4, RFP-hTSCs were seeded in the maternal compartment and maintained in iCTB media for 24 h. On day 5, perfusion was initiated for the GFP-HUVECs in the fetal compartment, using a peristaltic pump to deliver media at a flow rate of 3.5 μL/min. At this point (day 5), the media in the maternal compartment were replaced with forskolin-containing STB differentiation medium to induce the differentiation of hTSCs into STB, which continued for 3 days. Figure 4B features a fluorescence image of the tri-coculture system on day 6, *i.e.*, 24 h after syncytialization was initiated on the maternal side and overnight media perfusion began in the fetal microchannels. On day 8, the tri-coculture system was considered mature and ready for downstream viability and barrier function assays. 3D confocal microscopy reconstruction (Figure 4C) confirmed the layered architecture of our placental barrier model, revealing a dense, differentiated RFP-expressing STB layer overlaying the GelMA-encapsulated DiD-labeled PDSFs, while GFP-expressing HUVECs were clearly visible on the fetal side. Confocal images indicate good morphology across all cell types, with the STBs forming a compact layer on the GelMA surface (Figure S4).

3.5. Functional characterization of the tri-coculture model

Given the presence of three distinct cell types co-cultured within the same system, we were not able to measure the metabolic activity of each cell type individually. However, we assessed metabolic activity at the compartment level by comparing the maternal and fetal sides of the hPOC device. We used a commercially available colorimetric cell metabolic activity assay, CyQUANT Cell Proliferation Kit XTT Assay (Invitrogen, USA), which relies on the mitochondrial enzymes of live cells to convert the yellow XTT dye to an orange-colored compound called formazan. The absorbance of XTT increased over time in both compartments, albeit at a lower rate in the fetal compartment, potentially reflecting a lower overall cell number compared to the maternal compartment and the lower metabolic activity of endothelial cells compared to the highly metabolically active trophoblasts in the maternal compartment (Figure S5).

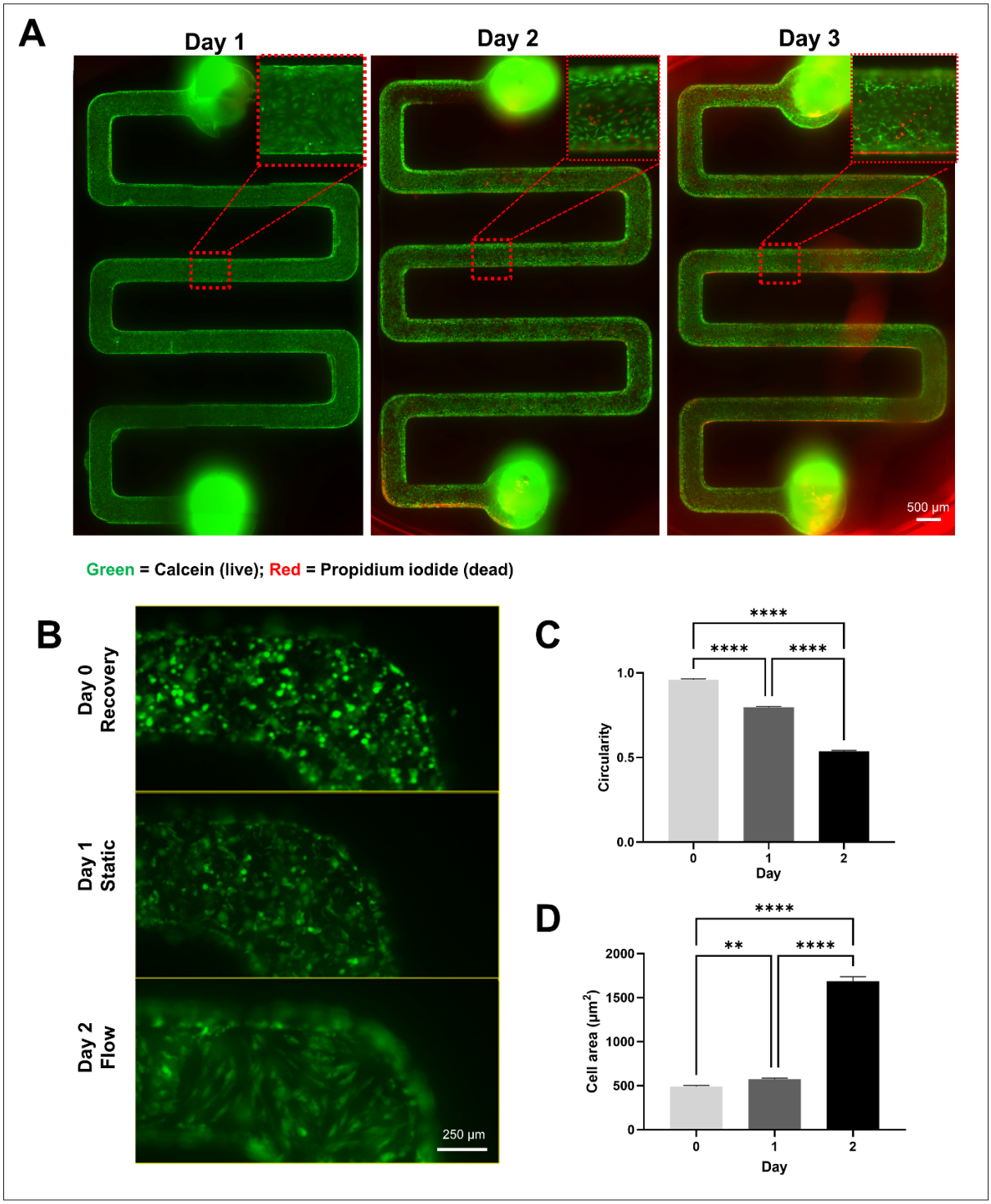

Figure 3. Optimization of HUVEC culture in the fetal compartment. (A) Live/dead staining of HUVECs seeded into microchannels (width: 500 µm) over 3 days of static culture, displaying high cell viability. (B) Morphological progression of GFP-HUVECs within the microchannels: cells exhibited a rounded morphology upon seeding, transitioned to a characteristic "cobblestone" appearance after 1 day of static culture, and adopted an elongated, striated morphology after 1 day of perfusion culture. (C) Quantification of GFP-HUVEC circularity reveals a significant decrease over the 2-day culture period (n = 3). Error bars indicate the SEM. (D) Cell area significantly increased following transition from static to dynamic (perfused) culture conditions (n = 3). Error bars indicate SEM. $^{**}p < 0.01$; $^{****}p < 0.0001$. Scale bars: 500 µm (A); 250 µm (B). Abbreviations: GFP, green fluorescent protein; HUVEC, human umbilical vein endothelial cells; SEM, standard error of the mean.

In the placenta, STB secretes several key hormones, including hCGβ, progesterone, estradiol, and hPL. To evaluate the functionality of the STB layer in our tri-coculture hPOC model, we collected media from both the maternal and fetal compartments every 24 h, starting on day 4 immediately after hTSC seeding, and assessed hormone levels using ELISA (Figure 4D–G).

Estradiol, a key steroid hormone involved in promoting trophoblast proliferation and differentiation into STBs,[31] was detected at high concentrations in the maternal compartment of the hPOC model as early as 1 day after the addition of forskolin, with levels remaining stable at ~20 ng/mL over the subsequent 3 days (Figure 4D). Similar to *in vivo* findings, where estradiol is also detected in the fetal circulation,[32] the spent media in the fetal compartment contained nearly 12 ng/mL estradiol 1 day after induction of syncytialization, with concentrations progressively increasing over the consecutive days.

hPL is a protein hormone secreted by the STB that plays key roles in regulating maternal metabolism and supporting fetal growth and development.[33] In our 3D hPOC model, hPL levels rose sharply in the maternal compartment 48 h after forskolin addition (*i.e.*, 3 days after hTSC seeding), but remained ~10-fold lower in the fetal compartment (Figure 4E).

hCGβ is a peptide hormone produced by the STB that reaches the fetal circulation primarily through passive diffusion.[34] In our tri-coculture model, the hCGβ concentration in the maternal compartment increased progressively each day following hTSC seeding, ranging from 6 to 15 μg/mL (Figure 4F). In contrast, hCGβ levels in the fetal compartment remained >100-fold lower, remaining below 200 ng/mL, consistent with limited diffusion across the placental barrier (Figure 4F).

Finally, progesterone is a steroid hormone with multiple roles in the maintenance of pregnancy, and it is typically found at markedly higher concentrations in the maternal circulation compared to the fetal circulation.[35] In our hPOC model, progesterone was detectable in the maternal compartment starting 1 day after hTSC seeding (Figure 4G), whereas levels in the fetal compartment remained below the assay's detection limit.

3.6. Evaluation of placental barrier integrity

To assess barrier integrity, we designed four configurations of the hPOC device for diffusion assays (Figure 5A). Type 1 was an acellular device; Type 2 included an acellular GelMA layer; Type 3 incorporated HUVECs on the fetal side; and Type 4 represented the full tri-coculture system on day 8, featuring the complete placental barrier.

To evaluate placental barrier function against passive diffusion, we used Na-F salt, a small-molecule fluorescent tracer (MW 376.3 g/mol) that is commonly employed to assess membrane permeability, including in blood-brain barrier models.[36] Due to its low MW and comparable size to sucrose (342.3 g/mol), Na-F serves as a representative probe for passive diffusion.[37,38] Na-F was introduced into the maternal compartment on day 8 of tri-coculture, and media samples from the fetal compartment were collected after 24 h (Figure 5B). A progressive decrease in fetal Na-F concentration was observed from Type 1 through Type 4 devices, with the full tri-coculture model (Type 4) exhibiting the lowest levels. These findings highlight the cumulative contribution of each component of the hPOC to the system's resistance to passive transfer of small, charged molecules.

To assess the barrier's ability to restrict the diffusion of large molecules, we used FITC-dextran, a high-MW, neutral fluorescent tracer. FITC-dextran-containing culture media were added to the maternal compartment on day 8 of the tri-coculture, and media from the fetal compartment were collected after 24 h. Among the four device configurations, the Type 4 tri-coculture model exhibited the lowest FITC-dextran level in the fetal compartment (Figure 5C), indicating superior resistance to large molecule penetration. We note that the difference between the Type 1 and Type 4 devices was approximately threefold for Na-F and 1.5-fold for FITC-dextran, demonstrating that the hPOC model is more effective at limiting diffusion of small, charged molecules than large, neutral molecules.

We also investigated the contributions of the acellular and cellular components of the hPOC device to active transport. In the placenta, glucose transport is primarily mediated by the GLUT1 transporter, a member of the glucose transporter (GLUT) family. To assess glucose dynamics in our model, we used physiologic glucose concentrations in both maternal and fetal compartments and monitored glucose levels in both compartments over time in the Type 1 and Type 4 devices. In the acellular device, the glucose concentration gradually decreased on the maternal side and correspondingly increased in the fetal side (Figure 5D), consistent with passive diffusion from a compartment with a higher concentration to one with a lower concentration. In contrast, in the tri-coculture system, maternal glucose concentration decreased dramatically within 1 h after the media was refreshed on both sides, while fetal glucose concentration increased gradually (**Figure 5E**). We postulate that the rapid decline in glucose concentration in the maternal compartment was

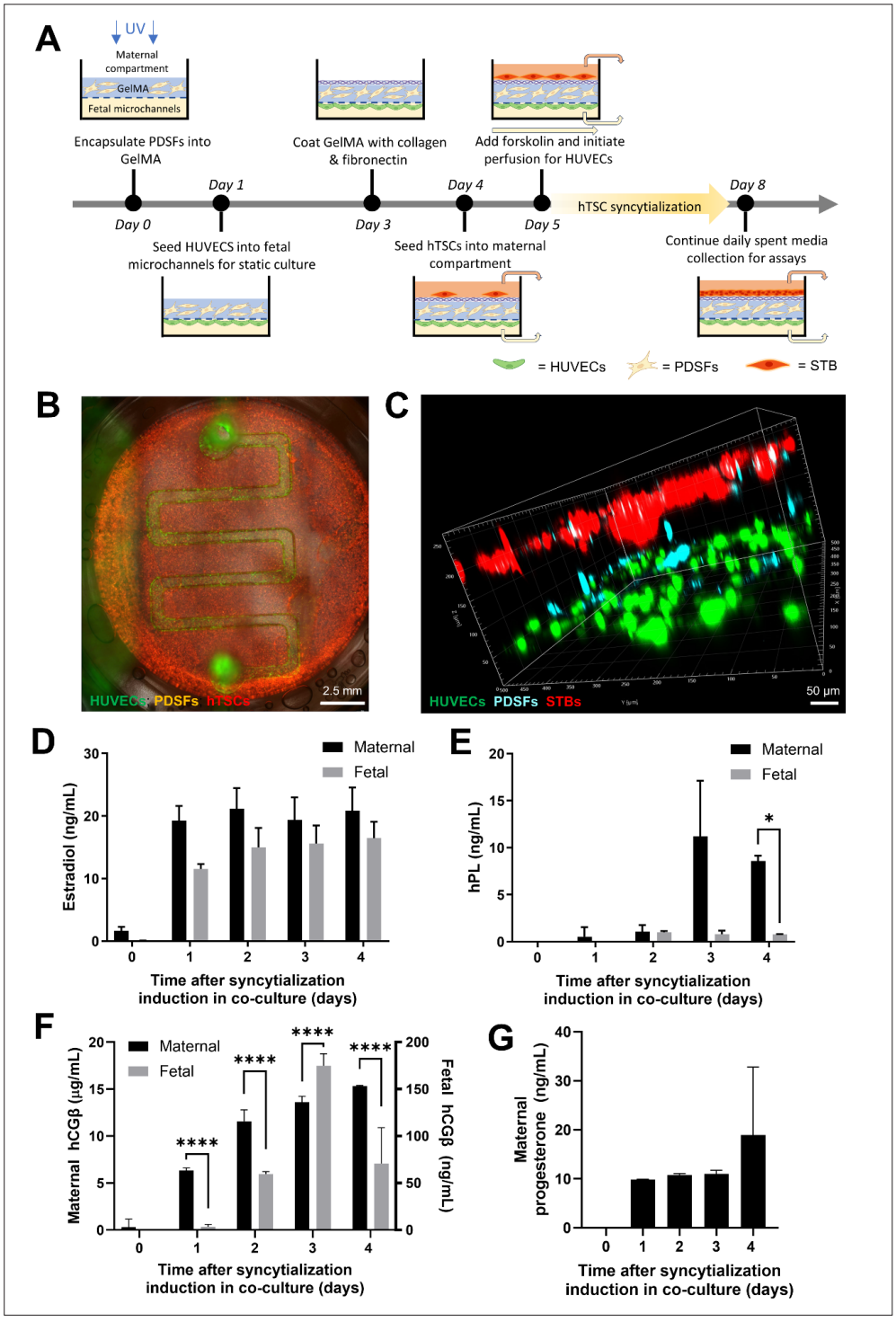

Figure 4. Assembly and functional characterization of the hPOC device. (A) Schematic timeline of assembling the tri-coculture placental model. (B) Composite fluorescence image of the tri-coculture model on day 6 (after 1 day of perfusion culture), featuring GFP-expressing HUVECs (green), DiD-labeled PDSFs (yellow), and RFP-expressing hTSCs (red). (C) 3D confocal reconstruction of the placental barrier on day 8 of tri-coculture, displaying the layered organization of STB, PDSFs, and HUVECs. (D–G) Hormone secretion assays measuring estradiol (D), hPL (E), hCGβ (F), and progesterone (G) levels over 4 days of forskolin treatment to induce syncytialization. Error bars indicate standard deviation of the mean ($n = 3$). Scale bars: 2.5 mm (B); 50 µm (C). *$p < 0.05$; ****$p < 0.0001$. Abbreviations: GelMA, methacrylated gelatin; GFP, green fluorescent protein; hPOC, human placenta-on-a-chip; hTSCs, human trophoblast stem cells; HUVECs, human umbilical vein endothelial cells; PDSFs, placenta-derived stromal fibroblasts; RFP, red fluorescent protein; STB, syncytiotrophoblast; hPL, human placental lactogen; hCGβ, beta subunit human chorionic gonadotropin.

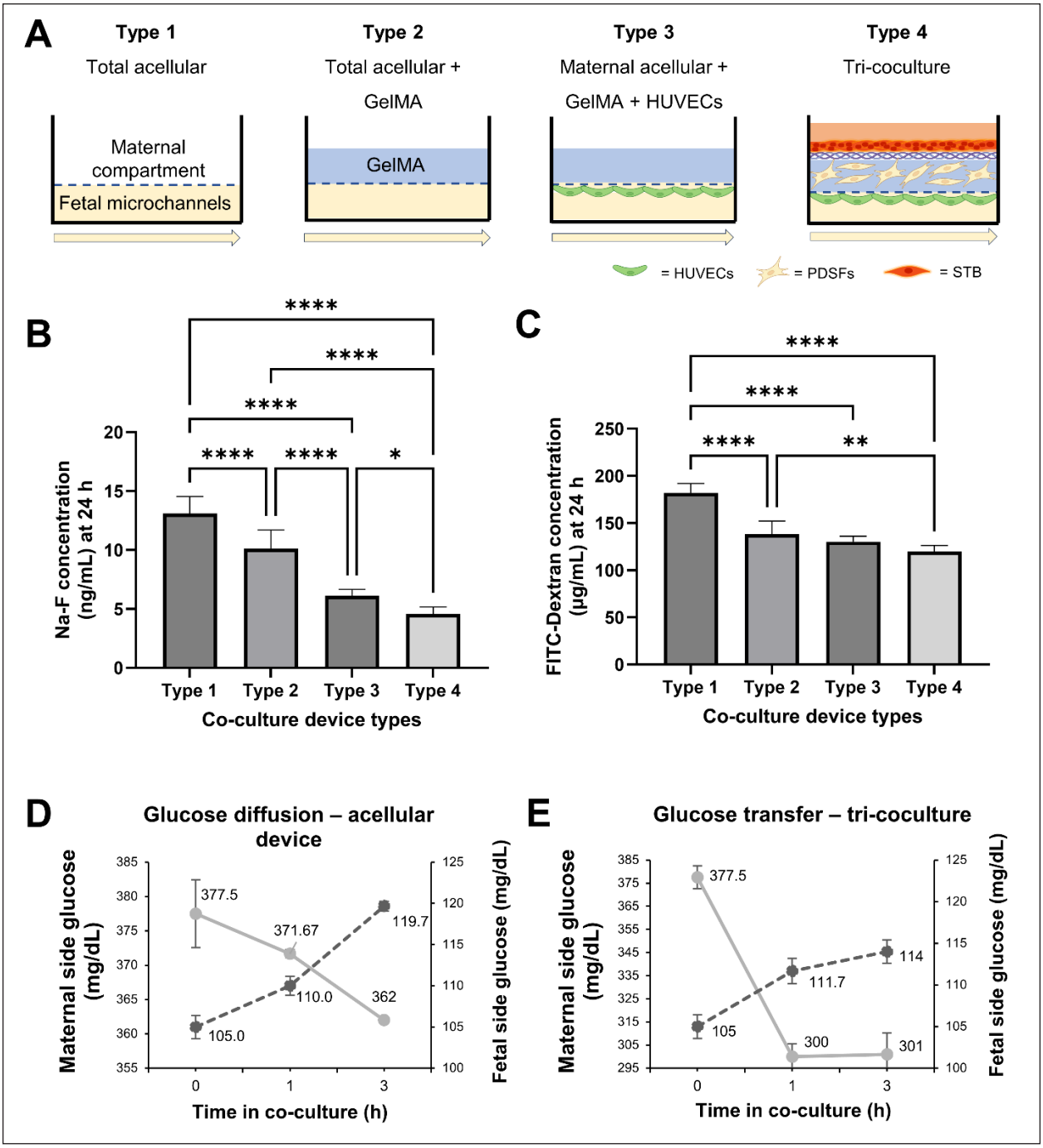

Figure 5. Assessment of placental barrier integrity in the hPOC model. (A) Schematic representation of the four hPOC devices used for barrier assays: Type 1 (fully acellular), Type 2 (acellular with GelMA layer), Type 3 (acellular GelMA layer on the maternal side; HUVECs on the fetal side), and Type 4 (full tri-coculture with GelMA-encapsulated PDSFs, STB, and HUVECs). (B) Sodium fluorescein (Na-F) penetration across the barrier displayed progressively lower fetal concentrations from Type 1 to Type 4, with the lowest leakage observed in the full tri-coculture system. Error bars indicate SD of the mean (n = 3). (C) FITC-dextran penetration was similarly reduced in the Type 4 device, indicating the model's ability to restrict the transport of large molecules. Error bars indicate SD of the mean (n = 3). (D) In the acellular device type, maternal glucose levels decreased gradually while fetal glucose increased over time, consistent with passive diffusion. (E) In the tri-coculture system, maternal glucose concentration dropped sharply within the first hour, suggesting high metabolic consumption by the STB layer; a corresponding but modest increase was observed on the fetal side. Error bars indicate SD of the mean (n = 3). *p < 0.05; **p < 0.01; ****p < 0.0001. Abbreviations: GelMA, methacrylated gelatin; hPOC, human placenta-on-a-chip; HUVECs, human umbilical vein endothelial cells; PDSFs, placenta-derived stromal fibroblasts; SD, standard deviation; STB, syncytiotrophoblast.

likely due to high metabolic consumption by STB, which is present at high cell density in the maternal compartment.

4. Discussion

In this study, we developed a hybrid open/closed microfluidic platform that enables both 3D cell encapsulation and 2D surface seeding. On the maternal side, we achieved 3D encapsulation of PDSFs and 2D seeding of hTSCs, while the fetal side mimics perfusable capillaries, where HUVECs are cultured to model the fetal endothelium. Compared to previous placenta-on-a-chip models that rely primarily on 2D cell seeding,[15,18,20,28] our design offers enhanced flexibility for recapitulating the complex 3D architecture of chorionic villi in the human placenta. To achieve precise structural control, we utilized DLP 3D printing to fabricate a multi-layered microfluidic device with customizable geometries and integrated features. Notably, the fetal-side channel was engineered with tunable dimensions to accommodate varying experimental requirements, highlighting the system's versatility. Beyond placental modeling, the modular and customizable nature of our platform renders it broadly applicable to other *in vitro* barrier models, including gut, lung, and blood–brain barrier systems, where spatial organization and compartment-specific cell interactions are critical.

The results from our tri-coculture hPOC device offer important insights into cellular interactions and barrier function that closely mimic the *in vivo* placental environment. All three cell types in the model exhibited excellent viability throughout the experimental timeline. All three primary cell types in the model maintained excellent viability throughout the 8-day culture period. Achieving this level of cellular performance required systematic optimization of multiple parameters to support the distinct requirements of each cell type. Specifically, we finetuned the substrate stiffness, coatings, and embedding methods to establish a stable and functional tri-culture system. Among these, the GelMA layer—which encapsulates PDSFs and supports hTSC seeding—was a key focus. We tested multiple stiffness levels and selected 18 kPa as the optimal stiffness based on cell viability, morphology, and structural integrity during culture. Although the reported stiffness of native placental tissue varies widely depending on anatomical region and measurement method, with values ranging from sub-kPa to as high as 30 kPa, we selected a range of GelMA stiffnesses spanning this spectrum to identify the optimal condition for cell performance.[19,39,40] Based on assessments of cell viability, morphology, and structural integrity, we chose 18 kPa as the final stiffness. This value not only falls within the broader physiological range but also supports robust growth and function of both PDSFs and hTSCs in our *in vitro* microfluidic setting. During the optimization of hTSC and HUVEC seeding, we found that surface coating with fibronectin and collagen was essential for promoting robust cell adhesion. In future iterations of the model, additional ECM components, such as fibronectin and laminin, could also be incorporated into the GelMA layer to further enhance cell viability, morphology, and function. On the fetal side, the flow rate of 3.5 μL/min was selected based on the channel size and the need for cell proliferation. While this rate generates wall shear stress lower than the 10 dyn/cm² observed in fetal capillaries *in vivo*,[41] it is closer to other placenta-on-a-chip models, which typically apply 0.5–2.5 μL/min to maintain cell viability, preserve barrier function, and prevent flow-induced damage.[20,42–44] This flow rate supports endothelial cell alignment and nutrient exchange while preserving the structural and functional integrity of the tri-culture model over extended culture periods. The metabolic activity assay demonstrated higher activity in the maternal compartment, likely due to the higher cell density and metabolic activity of hTSCs/STB relative to HUVECs on the fetal side.

In regard to placental hormone secretion, all four tested hormones were readily detected in the hPOC model. The observation that estradiol concentration was only slightly lower in the fetal compartment compared to the maternal compartment suggests that it is either secreted by both the apical and basal sides of the STB or secreted apically and readily transferred from the maternal to the fetal compartment. In contrast, the markedly lower levels of hPL, hCGβ, and progesterone in the fetal compartment suggest selective secretion of these hormones by the apical side of the STB, with limited transport across the placental barrier. Notably, we observed a plateau in maternal hCGβ levels over time, which aligns with the well-documented decline in hCGβ production as pregnancy advances.[45] The transient decrease in fetal hCGβ concentration on day 4 may reflect the progressive maturation of the fetomaternal barrier, potentially making it less permissive to hormone diffusion as syncytialization stabilizes. Although this interpretation remains speculative, it is consistent with the overall trend of functional barrier maturation observed throughout the 8-day culture period. These findings highlight the potential of the hPOC system to serve as a platform for future studies aimed at elucidating the mechanisms of placental hormone secretion and transport.

The diffusion assays using Na-F and FITC-dextran highlight the effectiveness of the tri-coculture model in recapitulating the selective permeability of the human

placental barrier. The progressive decrease in Na-F penetration across device types—from fully acellular to the tri-coculture system—demonstrates the critical role of cellular components in reinforcing barrier integrity against passive diffusion of small, charged molecules. Similarly, the marked reduction in FITC-dextran permeability in the tri-coculture device confirms the model's resistance to the passage of large, neutral molecules. Taken together, these findings validate the physiological relevance of the hPOC model and support its future application in pharmacological and toxicological studies of placental transport.

Physiological rates of glucose transfer across the human placenta over a 2 h period, as measured in *ex vivo* perfusion studies, range from 26.5 to 38.3%.[42,46] This transport is primarily mediated by the GLUT1 receptor on the STB and involves active, facilitated diffusion mechanisms.[47] In our hPOC model, glucose concentration in the fetal compartment increased similarly over time in both the acellular and tri-coculture systems. However, in the maternal compartment, the glucose concentration fell more rapidly and to a greater extent in the tri-coculture model, which we attribute to glucose consumption by the STB. The similarity in fetal glucose concentrations between the two systems (acellular and tri-coculture) limits our ability to distinguish whether the maternal-to-fetal compartment glucose transfer in the tri-coculture system is mediated by passive, facilitated, or active transport. Future studies are warranted to address this issue, potentially through the use of real-time glucose monitoring or by introducing a non-metabolizable glucose analog—such as 3-O-methyl-D-glucose—which is transported via GLUT1 but not metabolized, thereby enabling direct assessment of transcellular transport independent of cellular consumption.

Our hPOC model is designed to recapitulate key placental functions within a tractable experimental window. Therefore, we intentionally accelerated hTSC differentiation into STBs to enable functional assessment of hormone secretion and barrier function within an 8-day timeframe. In contrast to traditional placental explant cultures, which are often difficult to maintain beyond a few days due to declining viability and function,[4,48] our platform remained structurally intact and functionally active for at least 8 days, which is comparable to the culture durations reported for other placenta-on-a-chip systems.[43,49,50]

Overall, our study advances the understanding of placental barrier function and establishes a robust and modular platform for testing and developing therapeutic strategies relevant to pregnancy. While the hPOC device successfully recapitulates key structural and functional features of the human placenta, *in vitro* models inevitably face challenges in fully mimicking the complexity of the *in vivo* environment. Continued refinements in cell culture conditions, barrier composition, and transport dynamics will be critical to further improving the physiological relevance of the system.

Future studies should expand barrier integrity assessments by incorporating biologically relevant molecules or drugs beyond glucose. For example, insulin—an essential hormone for fetal growth—represents a particularly relevant candidate to test in conjunction with glucose to evaluate hormone-specific transport behavior. Likewise, evaluating the selective translocation of immunoglobulins could further validate the model's fidelity. Immunoglobulin G (IgG) is known to cross the placenta via FcRn-mediated transport in STB cells, whereas immunoglobulin M (IgM) does not.[51] Demonstrating the differential transport of IgG and IgM within the hPOC system would be a strong indicator of its physiological accuracy. In addition, future improvements to the model could include incorporating fetal Hofbauer cells into the stromal compartment and adjusting the distance between the maternal and fetal compartments—as well as modifying the trophoblast compartment—to better mimic the structure and transport characteristics of chorionic villi at distinct stages of gestation. In addition to assessing molecular transport across the platform, molecular profiling techniques, such as transcriptomic and metabolomic analyses, could be employed to comprehensively evaluate the physiological relevance of the model. It is worth noting that in our hPOC system, hTSCs are derived from early gestation, whereas PDSFs are isolated from the third-trimester placentas, resulting in a gestational age mismatch between the two cell types. While this approach is common due to the accessibility and stability of these cell sources, it may not fully capture the stage-specific cellular interactions of the native placenta. Protocols for deriving hTSCs from mid- to late-gestation placental tissues[24,25,52] could enable the development of gestational age-matched models that more accurately reflect the physiological state of the placenta at specific stages. Incorporating such advances into future versions of our model may enhance its relevance for studying stage-specific placental functions.

Further testing and optimization of this model will have important implications for the development of physiologically relevant *in vitro* models for understanding placental function. These advances will support deeper mechanistic studies of placental function, facilitate the assessment of environmental and pharmaceutical exposures during pregnancy, and enable safer therapeutic development for maternal-fetal health.

5. Conclusion

In this study, we have developed a biomimetic, microfluidic, tri-coculture 3D transport model that recapitulates key features of the human placenta. This model incorporates two primary placental tissue-derived cell types—hTSCs differentiated to STB facing the maternal compartment and PDSFs within a 3D stromal matrix—alongside HUVECs, a well-established endothelial model used to represent the fetal-facing vasculature. The microfluidic device's open-top design enables modular assembly of the maternal compartment—featuring a 2D layer of differentiated hTSCs layered atop a stiffness-tuned, GelMA-encapsulated 3D PDSF scaffold—while the closed fetal microchannel compartment supports perfusion flow and HUVEC seeding.

Our results demonstrate that the device sustains a viable tri-coculture system over multiple days, supports perfusion, and satisfies a critical requirement for *in vitro* placenta models: the formation of a functional, syncytialized layer of trophoblast that creates the tight barrier essential for proper placental function. Barrier formation was confirmed via microscopy, and functional validation was achieved through a variety of hormone secretion profiling and molecular transport assays.

This platform offers a robust and physiologically relevant system for studying placental transport in both normal and diseased conditions. Its modularity and cell-type specificity also provide opportunities to investigate genetic and environmental perturbations to better understand placental physiology and pathophysiology.

Acknowledgments

Figures 1A, 1D, 4A, and 5A partly feature schematics that were generated using BioRender (biorender.com) under an academic license. Additional customized schematics were added to the BioRender-generated images to complete the figures.

Funding

This work was supported in part by grants from the National Institutes of Health (NIH) to S.C., L.L., and M.P. (R21HD100132) and the National Science Foundation (NSF) to S.C. (2135720). The UCSD School of Medicine Microscopy Core facility was supported by the NIH grant P30 NS047101.

Conflict of interest

The authors declare no competing interests.

Author contributions

Conceptualization: Henry H. Hwang, Chandana Tekkatte, Louise C. Laurent, Shaochen Chen

Data curation: Yazhi Sun, Henry H. Hwang, Chandana Tekkatte, Scott A. Lindsay

Formal analysis: Yazhi Sun, Henry H. Hwang, Chandana Tekkatte, Scott A. Lindsay

Funding acquisition: Mana M. Parast, Louise C. Laurent, Shaochen Chen

Investigation: Yazhi Sun, Henry H. Hwang, Chandana Tekkatte, Scott A. Lindsay, Anelizze Castro-Martinez, Claire Yu, Isabella Saldana, Xuanyi Ma, Omar Farah

Methodology: Yazhi Sun, Henry H. Hwang, Chandana Tekkatte, Scott A. Lindsay, Anelizze Castro-Martinez, Claire Yu, Isabella Saldana, Xuanyi Ma, Omar Farah

Project administration: Louise C. Laurent, Shaochen Chen

Resources: Mana M. Parast, Louise C. Laurent, Shaochen Chen

Supervision: Louise C. Laurent, Shaochen Chen

Visualization: Yazhi Sun, Henry H. Hwang, Chandana Tekkatte, Scott A. Lindsay

Writing–original draft: Yazhi Sun, Henry H. Hwang, Chandana Tekkatte, Scott A. Lindsay,

Writing–review & editing: Mana M. Parast, Louise C. Laurent, Shaochen Chen

Ethics approval and consent to participate

The current study involving human-sourced tissues used in biomedical research was approved by the Institutional Review Board at the University of California San Diego (IRB #181917).

Consent for publication

Written informed consent was obtained from the donors to publish the data.

Availability of data

The data that support the findings of this study are available from the corresponding authors upon reasonable request.

References

1. Mitchell AA, Gilboa SM, Werler MM, Kelley KE, Louik C, Hernández-Díaz S. Medication use during pregnancy, with particular focus on prescription drugs: 1976–2008. *Am J Obstetr Gynecol.* 2011;205(1):51.e1-51.e8. doi: 10.1016/j.ajog.2011.02.029

2. Wesley BD, Sewell CA, Chang CY, Hatfield KP, Nguyen CP. Prescription medications for use in pregnancy–perspective from the US Food and Drug Administration. *Am J Obstetr Gynecol.* 2021;225(1):21-32.

doi: 10.1016/j.ajog.2021.02.032

3. Zubizarreta ME, Xiao S. Bioengineering models of female reproduction. *Bio Des Manuf*. 2020;3(3):237. doi: 10.1007/s42242-020-00082-8

4. Zabel RR, Favaro RR, Groten T, Brownbill P, Jones S. Ex vivo perfusion of the human placenta to investigate pregnancy pathologies. *Placenta*. 2022;130:1-8. doi: 10.1016/j.placenta.2022.10.006

5. Glättli SC, Elzinga FA, van der Bijl W, et al. Variability in perfusion conditions and set-up parameters used in *ex vivo* human placenta models: a literature review. *Placenta*. 2024;157:37-49. doi: 10.1016/j.placenta.2024.03.007

6. Carter AM. Animal models of human placentation – a review. *Placenta*. 2007;28:S41-S47. doi: 10.1016/j.placenta.2006.11.002

7. Carter AM. Evolution of placental hormones: implications for animal models. *Front Endocrinol*. 2022;13:891927. doi: 10.3389/fendo.2022.891927

8. Sood A, Kumar A, Gupta VK, Kim CM, Han SS. Translational nanomedicines across human reproductive organs modeling on microfluidic chips: state-of-the-art and future prospects. *ACS Biomater Sci Eng*. 2023;9(1):62-84. doi: 10.1021/acsbiomaterials.2c01080

9. Pu Y, Gingrich J, Veiga-Lopez A. A 3-dimensional microfluidic platform for modeling human extravillous trophoblast invasion and toxicological screening. *Lab Chip*. 2021;21(3):546-557. doi: 10.1039/D0LC01013H

10. Heaton SJ, Eady JJ, Parker ML, et al. The use of BeWo cells as an in vitro model for placental iron transport. *Am J Physiol Cell Physiol*. 2008;295(5):C1445-C1453. doi: 10.1152/ajpcell.00286.2008

11. Park JY, Mani S, Clair G, et al. A microphysiological model of human trophoblast invasion during implantation. *Nat Commun*. 2022;13(1):1252. doi: 10.1038/s41467-022-28663-4

12. Hori T, Okae H, Shibata S, et al. Trophoblast stem cell-based organoid models of the human placental barrier. *Nat Commun*. 2024;15(1):962. doi: 10.1038/s41467-024-45279-y

13. Kallol S, Moser-Haessig R, Ontsouka CE, Albrecht C. Comparative expression patterns of selected membrane transporters in differentiated BeWo and human primary trophoblast cells. *Placenta*. 2018;72-73:48-52. doi: 10.1016/j.placenta.2018.10.008

14. Cao R, Wang Y, Liu J, Rong L, Qin J. Self-assembled human placental model from trophoblast stem cells in a dynamic organ-on-a-chip system. *Cell Prolif*. 2023;56(5):e13469. doi: 10.1111/cpr.13469

15. Cao R, Guo Y, Liu J, et al. Assessment of nanotoxicity in a human placenta-on-a-chip from trophoblast stem cells. *Ecotoxicol Environ Saf*. 2024;285:117051. doi: 10.1016/j.ecoenv.2024.117051

16. Lermant A, Rabussier G, Davidson L, Lanz HL, Murdoch CE. Protocol for a placenta-on-a-chip model using trophoblasts differentiated from human induced pluripotent stem cells. *STAR Protoc*. 2024;5(1):102879. doi: 10.1016/j.xpro.2024.102879

17. Wang Y, Guo Y, Wang P, et al. An engineered human placental organoid microphysiological system in a vascular niche to model viral infection. *Commun Biol*. 2025;8(1):669. doi: 10.1038/s42003-025-08057-0

18. Pemathilaka RL, Caplin JD, Aykar SS, *et al*. Placenta-on-a-Chip: In Vitro Study of Caffeine Transport across Placental Barrier Using Liquid Chromatography Mass Spectrometry. *Global Challenges*. 2019;3(3):1800112. doi: 10.1002/gch2.201800112

19. Ma Z, Sagrillo-Fagundes L, Mok S, Vaillancourt C, Moraes C. Mechanobiological regulation of placental trophoblast fusion and function through extracellular matrix rigidity. *Sci Rep*. 2020;10(1):5837. doi: 10.1038/s41598-020-62659-8

20. Lee JS, Romero R, Han YM, et al. Placenta-on-a-chip: a novel platform to study the biology of the human placenta. *J Matern Fetal Neonatal Med*. 2016;29(7):1046-1054. doi: 10.3109/14767058.2015.1038518

21. Ma X, Yu C, Wang P, et al. Rapid 3D bioprinting of decellularized extracellular matrix with regionally varied mechanical properties and biomimetic microarchitecture. *Biomaterials*. 2018;185:310-321. doi: 10.1016/j.biomaterials.2018.09.026

22. Pyo SH, Wang P, Hwang HH, Zhu W, Warner J, Chen S. Continuous optical 3D printing of green aliphatic polyurethanes. *ACS Appl Mater Interfaces*. 2017;9(1):836-844. doi: 10.1021/acsami.6b12500

23. Igura K, Zhang X, Takahashi K, Mitsuru A, Yamaguchi S, Takahashi TA. Isolation and characterization of mesenchymal progenitor cells from chorionic villi of human placenta. *Cytotherapy*. 2004;6(6):543-553. doi: 10.1080/14653240410005366-1

24. Okae H, Toh H, Sato T, et al. Derivation of human trophoblast stem cells. *Cell Stem Cell*. 2018;22(1):50-63.e6. doi: 10.1016/j.stem.2017.11.004

25. Bai T, Peng CY, Aneas I, et al. Establishment of human induced trophoblast stem-like cells from term villous cytotrophoblasts. *Stem Cell Res*. 2021;56:102507. doi: 10.1016/j.scr.2021.102507

26. Zhu W, Qu X, Zhu J, et al. Direct 3D bioprinting of prevascularized tissue constructs with complex microarchitecture. *Biomaterials*. 2017;124:106-115.

doi: 10.1016/j.biomaterials.2017.01.042

27. Teasdale F. Gestational changes in the functional structure of the human placenta in relation to fetal growth: a morphometric study. *Am J Obstetr Gynecol*. 1980;137(5):560-568.
doi: 10.1016/0002-9378(80)90696-1

28. Blundell C, Yi YS, Ma L, et al. Placental drug transport-on-a-chip: a microengineered in vitro model of transporter-mediated drug efflux in the human placental barrier. *Adv Healthc Mater*. 2018;7(2):1700786.
doi: 10.1002/adhm.201700786

29. Wice B, Menton D, Geuze H, Schwartz AL. Modulators of cyclic AMP metabolism induce syncytiotrophoblast formation *in vitro*. *Exp Cell Res*. 1990;186(2):306-316.
doi: 10.1016/0014-4827(90)90310-7

30. Das S, Jegadeesan JT, Basu B. Gelatin methacryloyl (GelMA)-based biomaterial inks: process science for 3D/4D printing and current status. *Biomacromolecules*. 2024;25(4):2156-2221.
doi: 10.1021/acs.biomac.3c01271.

31. Tang C, Jin M, Ma B, et al. RGS2 promotes estradiol biosynthesis by trophoblasts during human pregnancy. *Exp Mol Med*. 2023;55(1):240-252.
doi: 10.1038/s12276-023-00927-z

32. Shutt DA, Smith ID, Shearman RP. Oestrone, oestradiol-17beta and oestriol levels in human foetal plasma during gestation and at term. *J Endocrinol*. 1974;60(2):333-341.
doi: 10.1677/joe.0.0600333

33. Johnson MS, Jackson DL, Schust DJ. Endocrinology of pregnancy. In: Skinner MK, ed. *Encyclopedia of Reproduction (Second Edition)*. Academic Press, Cambridge, MA, USA.; 2018:469-476.
doi: 10.1016/B978-0-12-801238-3.64672-X

34. Malek A, Sager R, Schneider H. Transport of proteins across the human placenta. *Am J Reprod Immunol*. 1998;40(5):347-351.
doi: 10.1111/j.1600-0897.1998.tb00064.x

35. Tal R, Taylor HS. Endocrinology of pregnancy. In: Feingold KR, Ahmed SF, Anawalt B, Blackman MR, Boyce A, Chrousos G, et al., eds. *Endotext*. MDText.com, Inc., South Dartmouth, MA, USA.; 2000.
http://www.ncbi.nlm.nih.gov/books/NBK278962/. Accessed May 15, 2025.

36. Kozler P, Pokorný J. Altered blood-brain barrier permeability and its effect on the distribution of Evans blue and sodium fluorescein in the rat brain applied by intracarotid injection. *Physiol Res*. 2003;52(5):607-14.
doi: 10.33549/physiolres.930289

37. Wevers NR, Nair AL, Fowke TM, et al. Modeling ischemic stroke in a triculture neurovascular unit on-a-chip. *Fluids Barriers CNS*. 2021;18(1):59.
doi: 10.1186/s12987-021-00294-9

38. Schaffenrath J, Huang SF, Wyss T, Delorenzi M, Keller A. Characterization of the blood–brain barrier in genetically diverse laboratory mouse strains. *Fluids Barriers CNS*. 2021;18(1):34.
doi: 10.1186/s12987-021-00269-w

39. Zambuto SG, Clancy KBH, Harley BAC. A gelatin hydrogel to study endometrial angiogenesis and trophoblast invasion. *Interface Focus*. 2019;9(5):20190016.
doi: 10.1098/rsfs.2019.0016

40. Kılıç F, Kayadibi Y, Yüksel MA, *et al*. Shear wave elastography of placenta: in vivo quantitation of placental elasticity in preeclampsia. *Diagn Interv Radiol*. 2015; 21(3):202-207.
doi: 10.5152/dir.2014.14338

41. Tarbell JM. Shear stress and the endothelial transport barrier. *Cardiovasc Res*. 2010;87(2):320-330.
doi: 10.1093/cvr/cvq146

42. Blundell C, Tess ER, Schanzer ASR, *et al*. A microphysiological model of the human placental barrier. *Lab Chip*. 2016;16(16):3065-3073.
doi: 10.1039/C6LC00259E

43. Boos JA, Misun PM, Brunoldi G, et al. Microfluidic co-culture platform to recapitulate the maternal–placental–embryonic axis. *Adv Biol*. 2021;5(8):2100609.
doi: 10.1002/adbi.202100609

44. Bhide A, Aboo A, Sawant M, Majumder A, Paul D, Modi D. Placenta on chip: a modern approach to probe feto-maternal interface. In: Mohanan PV, ed. *Microfluidics and Multi Organs on Chip*. Springer Nature, Singapore.; 2022:359-380.
doi: 10.1007/978-981-19-1379-2_16

45. Cole LA. Biological functions of hCG and hCG-related molecules. *Reprod Biol Endocrinol*. 2010;8(1):102.
doi: 10.1186/1477-7827-8-102

46. Brandes JM, Tavoloni N, Potter BJ, Sarkozi L, Shepard MD, Berk PD. A new recycling technique for human placental cotyledon perfusion: Application to studies of the fetomaternal transfer of glucose, inulin, and antipyrine. *Am J Obstetr Gynecol*. 1983;146(7):800-806.
doi: 10.1016/0002-9378(83)91081-5

47. Hahn T, Barth S, Weiss U, Mosgoeller W, Desoye G. Sustained hyperglycemia in vitro down-regulates the GLUT1 glucose transport system of cultured human term placental trophoblast: a mechanism to protect fetal development? *FASEB J*. 1998;12(12):1221-1231.
doi: 10.1096/fasebj.12.12.1221

48. Brownbill P, Sebire N, McGillick EV, Ellery S, Murthi P. Ex vivo dual perfusion of the human placenta: disease simulation, therapeutic pharmacokinetics and analysis of off-target effects. In: Murthi P, Vaillancourt C, eds. *Preeclampsia: Methods and Protocols*. Springer, New York, NY, USA.; 2018:173-189.

doi: 10.1007/978-1-4939-7498-6_14

49. Kouthouridis S, Saha P, Ludlow M, N. Truong BY, Zhang B. Late-stage placental barrier model for transport studies of prescription drugs during pregnancy. *Lab Chip*. 2025;25(13):3168-3184.
doi: 10.1039/D5LC00075K

50. Rabussier G, Bünter I, Bouwhuis J, et al. Healthy and diseased placental barrier on-a-chip models suitable for standardized studies. *Acta Biomater*. 2023;164:363-376.
doi: 10.1016/j.actbio.2023.04.033

51. Palmeira P, Quinello C, Silveira-Lessa AL, Zago CA, Carneiro-Sampaio M. IgG placental transfer in healthy and pathological pregnancies. *J Immunol Res*. 2012;2012(1):985646.
doi: 10.1155/2012/985646

52. Karakis V, Britt JW, Jabeen M, San Miguel A, Rao BM. Derivation of human trophoblast stem cells from placentas at birth. *J Biol Chem*. 2025;301(6):108505.
doi: 10.1016/j.jbc.2025.108505